Marjanović M, Vuksanović Dj. Linear Analysis of Single Delamination in Laminated Composite Plate using Layerwise Plate Theory. 4th International Congress of Serbian Society of Mechanics. Vrnjačka Banja, Serbia, 04-07.06.2013., 443-448. ISBN 978-86-909973-5-0

LINEAR ANALYSIS OF SINGLE DELAMINATION IN LAMINATED COMPOSITE PLATE USING LAYERWISE PLATE THEORY

Miroslav Marjanović[1], Đorđe Vuksanović[2]

[1] Faculty of Civil Engineering,
University of Belgrade, Bulevar kralja Aleksandra 73, 11000 Belgrade, Serbia
e-mail: mmarjanovic@grf.bg.ac.rs
[2] Faculty of Civil Engineering,
University of Belgrade, Bulevar kralja Aleksandra 73, 11000 Belgrade, Serbia
e-mail: george@grf.bg.ac.rs

Abstract. Composite materials have the important applications in the automotive and aircraft industry, shipbuilding, civil engineering etc. Plate damages usually appear at local (single layer) level. One of the most common forms of damage is delamination. For this reason, it is of interest to develop the layerwise plate theories, which are capable to describe the plate kinematics for each layer individually. This paper presents extended General Layerwise Theory, with emphasis on the analysis of delamination. The response of cracked plate is given through Displacement Control analysis. Four-noded 2D FE is formulated. Layerwise FE described in this paper allows independent interpolation of displacements through the plate thickness and in-plane. 2D crack propagation criteria are based on the LEFM. The usefulness of the proposed FE is verified by comparison with analytical solution.

1. Introduction

Analysis of laminar composites attracted the attention of many authors from different fields. Different plate theories have been developed - equivalent single layer, zig-zag theories, or **layerwise** theories. Great chapter in the analysis of the composite laminates is the influence of delamination in composite plate. It is well-known that during the manufacturing process, as well as from the impact forces and effects during the exploitation period, the damage in laminar composite can often occur. Due to the presence of these often microscopic structural defects, its loading capacity is reduced. An extensive overview of delamination problem can be found in [2-5, 12]. Once the delamination occurs in composite plate, its growth is usually predicted using LEFM criteria. The total strain energy release rate is divided in three components, as shown in Fig. 1. In order to predict delamination onset or growth, these calculated G components are compared to interlaminar fracture toughness. Experimentally obtai-ned critical ERR for all modes serve as a criterion for crack growth. In this work, ERR calculation based on the VCCT is performed with the fixed FE mesh, through algorithm explained in [6-7].

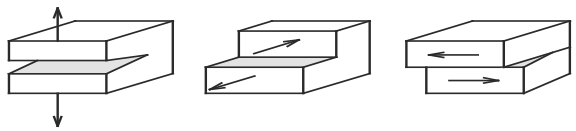

Figure 1. Different damage modes in laminar composite

2. Generalized Laminated Plate Theory

We will consider an orthotropic plate, composed from **n** orthotropic material layers (laminas), in global coordinate system, as shown on Fig. 2. To obtain smooth distribution of displacements through the thickness of the plate (cross-sectional warping), subdivisions through the plate thickness are introduced. In this way, polynomial degree of interpolation through the thickness is set. For the purpose of this work, linear *z*-interpolation is chosen.

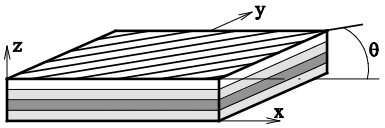

Figure 2. Laminated composite plate (4 layers) in global CS

$$u_1(x,y,z) = u(x,y) + \sum_{I=1}^{N} u^I(x,y)\Phi^I(z) + \sum_{I=1}^{ND} U^I(x,y)H^I(z)$$
$$u_2(x,y,z) = v(x,y) + \sum_{I=1}^{N} v^I(x,y)\Phi^I(z) + \sum_{I=1}^{ND} V^I(x,y)H^I(z)$$
$$u_3(x,y,z) = w(x,y) + \sum_{I=1}^{ND} W^I(x,y)H^I(z) \tag{1}$$

Delamination kinematics can be modeled using **GLPT** by introducing the set of delamination variables in displacement field expansion. These new displacement components represent the jump discontinuities in displacements in three orthogonal directions. Displacement components (u_1, u_2, u_3) at the (x, y, z) are assumed as shown in (1). (*u, v, w*) are mid-plane displacements, (u^I, v^I, w^I) are the nodal values of u_1, u_2 and u_3 in I^{th} numerical layer, and (U^I, V^I, W^I) are the jump discontinuities of u_1, u_2 and u_3 at delamination interface. N is the number of nodes through thickness of the laminate and ND is the number of numerical layers through the thickness in which delamination occurs. $\Phi^I(x,y)$ are the global interpolation functions for the discretization of in-plane displacements through the plate thickness. These functions are in detail given in [8]. $H^I(z)$ are the Heaviside step functions. $H^I(z) = 1$ for $z \geq z^I$ and $H^I(z) = 0$ for $z < z^I$. Some improvements of H^I in displacements expansion can be found in [9]. The variable W^I is Crack Opening Displacement (COD), thus the condition $W^I \geq 0$ denotes no-penetration condition for I^{th} delaminated surfaces. The delamination front is the node-wise curve in the delamination plane, along which essential boundary conditions $U^I = V^I = W^I = 0$ are enforced.

Linear kinematic relations associated with displacement field (1) are given in (2):

$$\varepsilon_x = \frac{\partial u_1}{\partial x}, \quad \varepsilon_y = \frac{\partial u_2}{\partial y}, \quad \gamma_{yz} = \frac{\partial u_2}{\partial z} + \frac{\partial u_3}{\partial y}, \quad \gamma_{xz} = \frac{\partial u_1}{\partial z} + \frac{\partial u_3}{\partial x}, \quad \gamma_{xy} = \frac{\partial u_1}{\partial y} + \frac{\partial u_2}{\partial x} \tag{2}$$

Displacements are continuous at the layer interfaces, except in the delaminated layer. Strains are discontinuous because of the layerwise definition of $\Phi^I(x,y)$. For linear elastic material that follows Hook-s law, constitutive equations for k^{th} lamina can be found in [8].

After substitution of stress resultants into the principle of virtual displacements, with homogenous BC, equilibrium equations are derived in following equation (3):

$$\delta U = \int_{\Omega} \left\{ \begin{array}{l} N_x \dfrac{\partial \delta u}{\partial x} + N_y \dfrac{\partial \delta v}{\partial y} + N_{xy} \left(\dfrac{\partial \delta u}{\partial y} + \dfrac{\partial \delta v}{\partial x} \right) + Q_x \dfrac{\partial \delta w}{\partial x} + Q_y \dfrac{\partial \delta w}{\partial y} + \\ + \sum_{I=1}^{N} \left(N_x^I \dfrac{\partial \delta u^I}{\partial x} + N_y^I \dfrac{\partial \delta v^I}{\partial y} + N_{xy}^I \left(\dfrac{\partial \delta u^I}{\partial y} + \dfrac{\partial \delta v^I}{\partial x} \right) + Q_x^I \delta u^I + Q_y^I \delta v^I \right) + \\ + \sum_{I=1}^{ND} \left(\bar{N}_x^I \dfrac{\partial \delta U^I}{\partial x} + \bar{N}_y^I \dfrac{\partial \delta V^I}{\partial y} + \bar{N}_{xy}^I \left(\dfrac{\partial \delta U^I}{\partial y} + \dfrac{\partial \delta V^I}{\partial x} \right) + \bar{Q}_x^I \dfrac{\partial \delta W^I}{\partial x} + \bar{Q}_y^I \dfrac{\partial \delta W^I}{\partial y} \right) \end{array} \right\} d\Omega$$

$$\delta V = -\int_{\Omega} \left(q \delta w \right) d\Omega \tag{3}$$

Stress resultants $\{N\}$, $\{N^I\}$ and $\{\bar{N}^I\}$ are obtained after integration of products of stress components and appropriate functions of z-coordinate for each lamina. These resultants are given in detail in Ćetković, Vuksanović [1] and Reddy [8]. Constitutive matrices of laminate used in (4) are given in works of Barbero and Reddy [5]. After that, laminate constitutive equations are derived by integrating stress resultants through the plate thickness:

$$\begin{aligned} \{N\} &= [A]\{\varepsilon\} + \sum_{I=1}^{N} \left[B^I \right] \{\varepsilon^I\} + \sum_{I=1}^{ND} \left[E^I \right] \{\bar{\varepsilon}^I\} \\ \{N^I\} &= \left[B^I \right] \{\varepsilon\} + \sum_{J=1}^{N} \left[D^{IJ} \right] \{\varepsilon^J\} + \sum_{J=1}^{ND} \left[L^{IJ} \right] \{\bar{\varepsilon}^J\} \\ \{\bar{N}^I\} &= \left[E^I \right] \{\varepsilon\} + \sum_{J=1}^{N} \left[L^{JI} \right] \{\varepsilon^J\} + \sum_{J=1}^{ND} \left[F^{IJ} \right] \{\bar{\varepsilon}^J\} \end{aligned} \tag{4}$$

3. Layerwise FE Model – Assumptions, Displacement Field and Stiffness Matrix

FE model consists of the middle plane, N numerical layers through plate thickness (excepting middle plane) and ND numerical layers in which delamination exist. Node variables are componentional translations and jump discontinuities in three orthogonal directions. Generalized displacements satisfy C^0 continuity conditions on element boundaries. Displacement field is interpolated using the Lagrangian interpolation functions:

$$\left(u, v, w, u^I, v^I, U^I, V^I, W^I \right) = \sum_{i=1}^{m} \left(u_i, v_i, w_i, u_i^I, v_i^I, U_i^I, V_i^I, W_i^I \right) \psi_i \tag{5}$$

In (13), $u_i, v_i, w_i, u_i^I, v_i^I, U_i^I, V_i^I, W_i^I$ are nodal values of the $u, v, w, u^I, v^I, U^I, V^I, W^I$. Index m denotes the number of nodes per element. For this purpose, four-node Lagrange quadrilateral is chosen. Interpolation is obtained using standard 2D Lagrangian polynomials. If we incorporate (5) into the virtual work principle (3), we will derive equilibrium equations of single FE in matrix form. It is now possible to derive the stiffness matrix of the single FE, with delamination variables taken into account. Submatrices of the proposed FE model are:

$$K_{11} = \int_{\Omega} [B]^T [A][B] d\Omega \qquad K_{12}^I = \int_{\Omega} [B]^T \left[B^I \right] \left[\bar{B} \right] d\Omega \qquad K_{13}^I = \int_{\Omega} [B]^T \left[E^I \right] [B] d\Omega$$

$$K_{21}^{I}=\int_{\Omega}\left[\overline{B}\right]^{T}\left[B^{I}\right]\left[B\right]d\Omega \qquad K_{22}^{IJ}=\int_{\Omega}\left[\overline{B}\right]^{T}\left[D^{IJ}\right]\left[\overline{B}\right]d\Omega \qquad K_{23}^{IJ}=\int_{\Omega}\left[\overline{B}\right]^{T}\left[L^{IJ}\right]\left[B\right]d\Omega$$

$$K_{31}^{I}=\int_{\Omega}\left[B\right]^{T}\left[E^{I}\right]\left[B\right]d\Omega \qquad K_{32}^{IJ}=\int_{\Omega}\left[B\right]^{T}\left[L^{JI}\right]\left[\overline{B}\right]d\Omega \qquad K_{33}^{IJ}=\int_{\Omega}\left[B\right]^{T}\left[F^{IJ}\right]\left[B\right]d\Omega$$

In previous expressions, $[B]$ and $[\overline{B}]$ are typical kinematic matrices, derived by appropriate differentiation of shape functions matrix. They are in detail given in [1]. Unknown displacements are then derived in a usual manner using standard FE procedure. Layerwise elements suffer from the phenomena such as spurious shear stiffness. Because of this, Selective integration is used to avoid the shear locking, in a thin plate situation. All members in the stiffness matrix are calculated using 2×2 or 1×1 points of Gauss-Legendre quadrature. Three different schemes of numerical integration are applied, as shown in 5.1.1.

4. Progressive Delamination

Once the delamination occurs, its growth is predicted by the fracture criterion. Griffith [10] proposed a criterion for a crack extension using the principle of minimum total potential energy. It has been improved by Rice [11] who postulated a contour integral that is path independent as the change in potential energy for a virtual crack extension (J-integral). In this paper, crack front shape is digitalized using a rectangular coordinate system [6-7]. Stationary mesh is used in all loading steps. Displacement field obtained from the FE analysis is then used for calculation of the Modes I-III of the SERR (G_I, G_{II} and G_{III}), using VCCT. In this work, algorithm is extended for nodes on the plate boundaries, by calculating unity vectors in which direction crack will grow. In the case of 4-node FE, ERR is a product of crack-tip-nodal-force and jump displacement behind the crack tip [3]. Once the G is calculated, a mixed mode fracture criterion, used to predict crack growth, is given in (6). G_{iC} are the critical values of ERR in all three modes, and they are assumed to be constant during crack growth. The exponents α,β,γ are equal to 1. Whole FE procedure, as well as the algorithm for calculation the G components, is coded using MATLAB®.

$$E_d=\left(\frac{G_I}{G_{IC}}\right)^{\alpha}+\left(\frac{G_{II}}{G_{IIC}}\right)^{\beta}+\left(\frac{G_{III}}{G_{IIIC}}\right)^{\gamma} \tag{6}$$

5. Numerical Example - Double Cantilever Beam (DCB) Problem

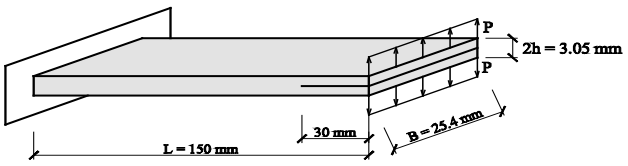

Figure 3. Double Cantilever Beam Model

The geometry and the loading of the DCB specimen are shown in Fig. 3. The T300/976 graphite/epoxy material is used, as in example [7]. Material properties are listed in Table 1. The fibers are oriented in specimen's longitudinal direction. As mentioned before, crack

front is generated by setting delamination variables U^I, V^I and W^I to zero. For this purpose, it is assumed that single delamination exists in the mid-plane of the 2-layer plate.

E_{11} [N/mm^2]	$E_{22} = E_{33}$ [N/mm^2]	$G_{12} = G_{13}$ [N/mm^2]	G_{23} [N/mm^2]
139300	**9720**	**5580**	**3450**
G_{Ic} [N/mm]	G_{IIc} [N/mm]	$\nu_{12} = \nu_{13}$ [-]	$\nu_{12} = \nu_{13}$ [-]
0.0876	**0.3152**	**0.29**	**0.29**

Table 1. Material properties of T300/976

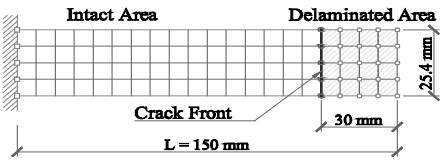

Figure 4. Finite Element Mesh (20 × 4)

5. 1 Influence of Integration Scheme. Mesh Refinement. Energy Release Rate distribution

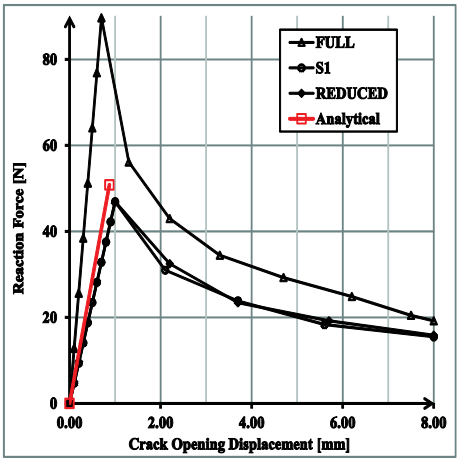

Figure 5. Reaction force versus COD for different schemes of selective integration (10×10 FE)

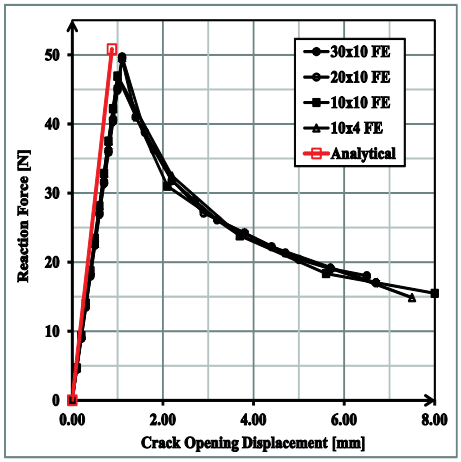

Figure 6. Reaction force versus COD for different FE meshes (S1 Integration Scheme)

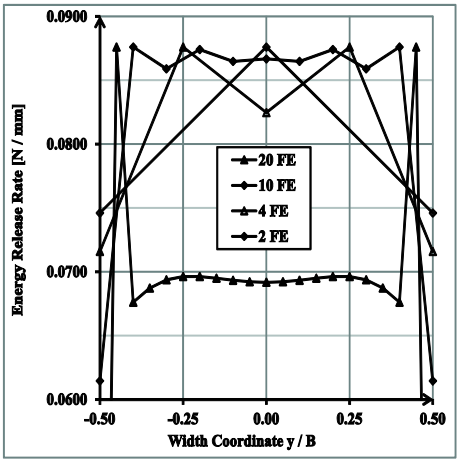

Figure 7. ERR Distribution over the width of the DCB in the moment of fracture (S1 Integration Scheme)

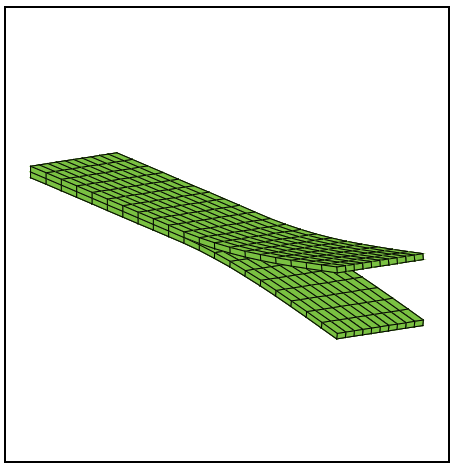

Figure 8. Deformed shape of DCB model during delamination propagation

Fig. 5 shows results obtained using different schemes of integration for calculation of element stiffness matrix. It is obvious that use of Full integration gives much stiffer response. After analyzing of mesh refinement, minimal discrepancy is obtained even for the coarse mesh. Results are compared with analytical solution, which can be found in [12].

Refinement of the FE mesh in width direction influences the results in a way that ERR distribution over the plate width changes significantly. As shown in Fig. 7, larger number of elements through the width leads to the constant distribution of ERR, only with one peak near the boundary, which can be neglected. S1 selective integration is used. Nodes with max ERR are first released in Displacement Control Exp.

6. Conclusions

Extended Generalized Laminated Plate Theory is presented. Numerical model using isoparametric FE is derived. Algorithm for derivation of crack front and calculation of ERR components is applied. Applicability of the theory is validated using an example of DCB, which is compared with analytical solution. Discrepancies with results from [7] are found because of the use of rigid interface law in this work, which will be further improved.

From previous example it is obvious that Selective Integration is necessary for calculation of element stiffness matrix. Mesh refinement in longitudinal direction does not affect the results of calculation severely, but refinement in lateral direction is important for calculation of ERR distribution through the width of the plate. Fine mesh is needed for smooth distribution of ERR in lateral direction.

Acknowledgement. The financial support of the Government of the Republic of Serbia - Ministry of Education and Science (Project TR-36048), is gratefully acknowledged.

References

[1] Ćetković M., Vuksanović Đ. (2009) Bending, free vibrations and buckling of laminated composite and sandwich plates using a layerwise displacement model, *Composite Structures*, **88**, pp. 219-227.
[2] Bolotin V. (1996) Delamination in composite structures: its origin, buckling, growth and stability, *Composites: Part B: Engineering*, **27**, pp. 129-145.
[3] Krueger R. (2004) The Virtual Crack Closure Technique: History, Approach and Applications, *Applied Mechanics Reviews*, **57**, pp. 109-143.
[4] O'Brien T. K. (1982) Characterization of Delamination Onset and Growth in a Composite Laminate, *Damage in Composite Materials, Reifsnider K. L. (ed.)*, STP 775, ASTM, Philadelphia, pp. 140-167.
[5] Barbero E. J., Reddy J. N. (1991) Modeling of delamination in composite laminates using a layer-wise plate theory, *International Journal of Solids and Structures*, **28**, pp. 373-388.
[6] Xie D., Biggers Jr. S. B. (2006) Strain energy release rate calculation for a moving delamination front of arbitrary shape based on the virtual crack closure technique. Part I: Formulation and validation, *Engineering Fracture Mechanics*, **73**, pp. 771-785.
[7] Hosseini-Toudeshky H., Hosseini S., Mohammadi B. (2010) Progressive delamination growth analysis using discontinuous layered element, *Composite Structures*, **92**, pp. 883-890.
[8] Reddy J. N. *Mechanics of Laminated Composite Plates: Theory and Analysis*. CRC Press, 1997.
[9] Zhang Y., Wang S. (2009) Buckling, post-buckling and delamination propagation in debonded composite laminates. Part 1: Theoretical development, *Composite Structures*, **88**, pp. 121-130.
[10] Griffith A. A. (1921) The Phenomena of Rupture and Flow in Solids, *Philosophical Transactions of the Royal Society of London. Series A,* **221**, pp. 163-198.
[11] Rice J. R. (1968) A Path Independent Integral and the Approximate Analysis of Strain Concentrations by Notches and Cracks, *Journal of Applied Mechanics*, **35**, pp. 379-386.
[12] Šumarac D., Krajčinović D. *Osnovi mehanike loma*. Naučna knjiga. Belgrade, 1990. (in serbian)